Figure S1

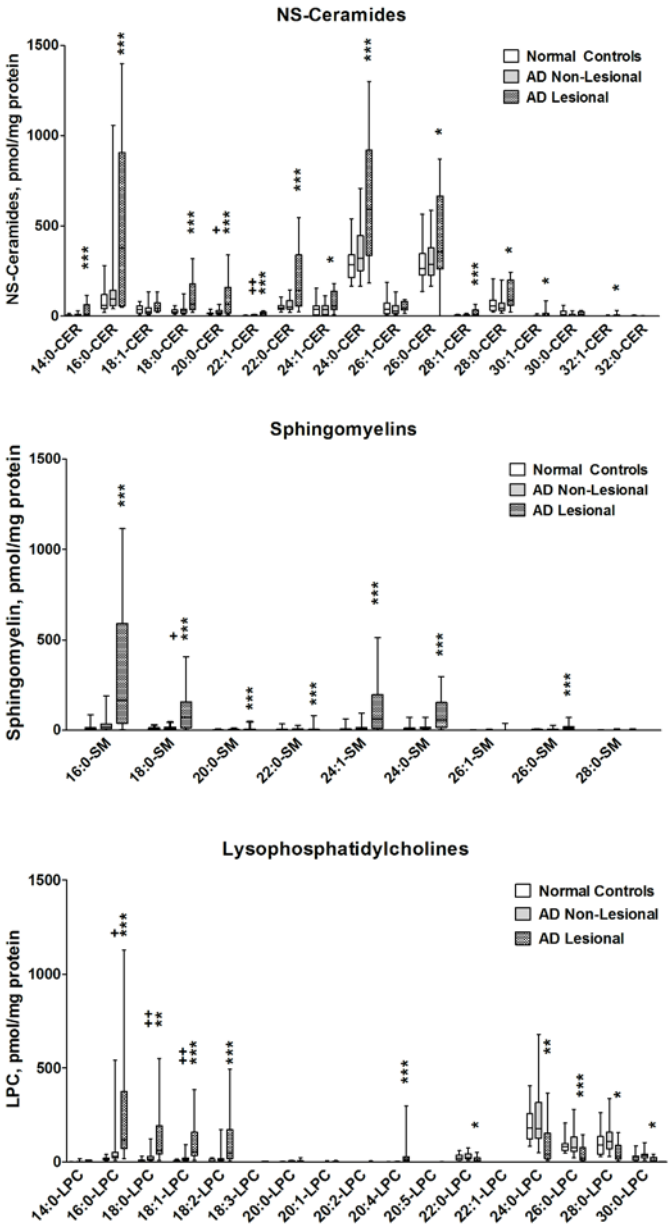

Figure S1. Changes in the absolute level of short- and long-chain molecular species in ceramides (**A**), sphingomyelins (**B**), and LPC (**C**) in *stratum corneum* of AD patients. Each lipid molecular specie was quantified by targeted LC-ESI-MS/MS and normalized by sample total protein content. Note that total level of lysophosphatidylcholines does not change, however the redistribution of the amounts of short and long-chain species is observed, this process is already pronounced in AD non-lesional skin. Data are presented as Whiskers plot with minimum and maximum values. $^{*,+}$ $p < 0.5$, $^{**,++}$ $p < 0.01$, $^{***,+++}$ $p < 0.001$ as compared to corresponding Normal Controls (two-tailed Studet's *t*-test). AD lesional skin – n=15, AD non-lesional skin – n=30, Normal Controls skin – n=25.

Figure S2

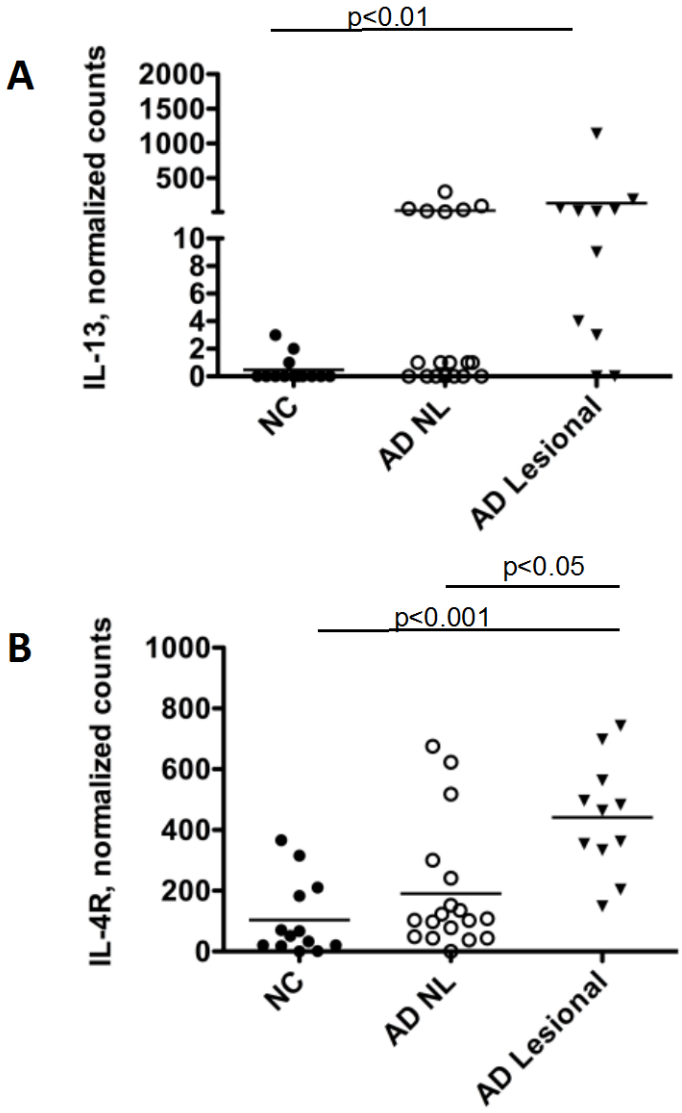

Figure S2. Increased expression of IL-13 (**A**) and IL-4R (**B**) in skin tape strip RNA samples collected from AD lesional and AD non-lesional skin as detected by RNAseq analysis of the skin tape strips. AD lesional skin – n=12, AD non-lesional skin – n=18, NC skin – n=13. The significance of difference between groups was determined using two-tailed Student's *t*-test.

Figure S3

LCBs \ FAs	Non-hydroxy FA (N)	α-hydroxy FA (A)	Esterified ω-hydroxy FA (EO)
Dihydro-Sph (DS)	NDS	ADS	EODS
Sph (S)	NS	AS	EOS
Phyto-Sph (P)	NP	AP	EOP
6-OH-Sph (H)	NH	AH	EOH

Figure S3. Classification of skin ceramides. Skin ceramides are classified based on their sphingoid bases (LCBs) and fatty acids (FAs) that *N*-acylate sphingoid base. Sphingoid bases can be sphingosine (S), dihydrosphingosine (DS), phytosphingosine (P), and 6-hydroxy-sphingosine (H). Fatty acids can be non-hydroxy (N) and alfa-hydroxy (A). A separate class of omega-esterified (EO) ceramides provides final four groups of ceramide subclasses based on sphingoid base in their structure (EOS, EODS, EOP, EOH). Current classification can be further extended based of the chain length of sphingoid base (in human skin, sphingoid bases with 18, 20, and 22 carbons are common).

Figure S4.

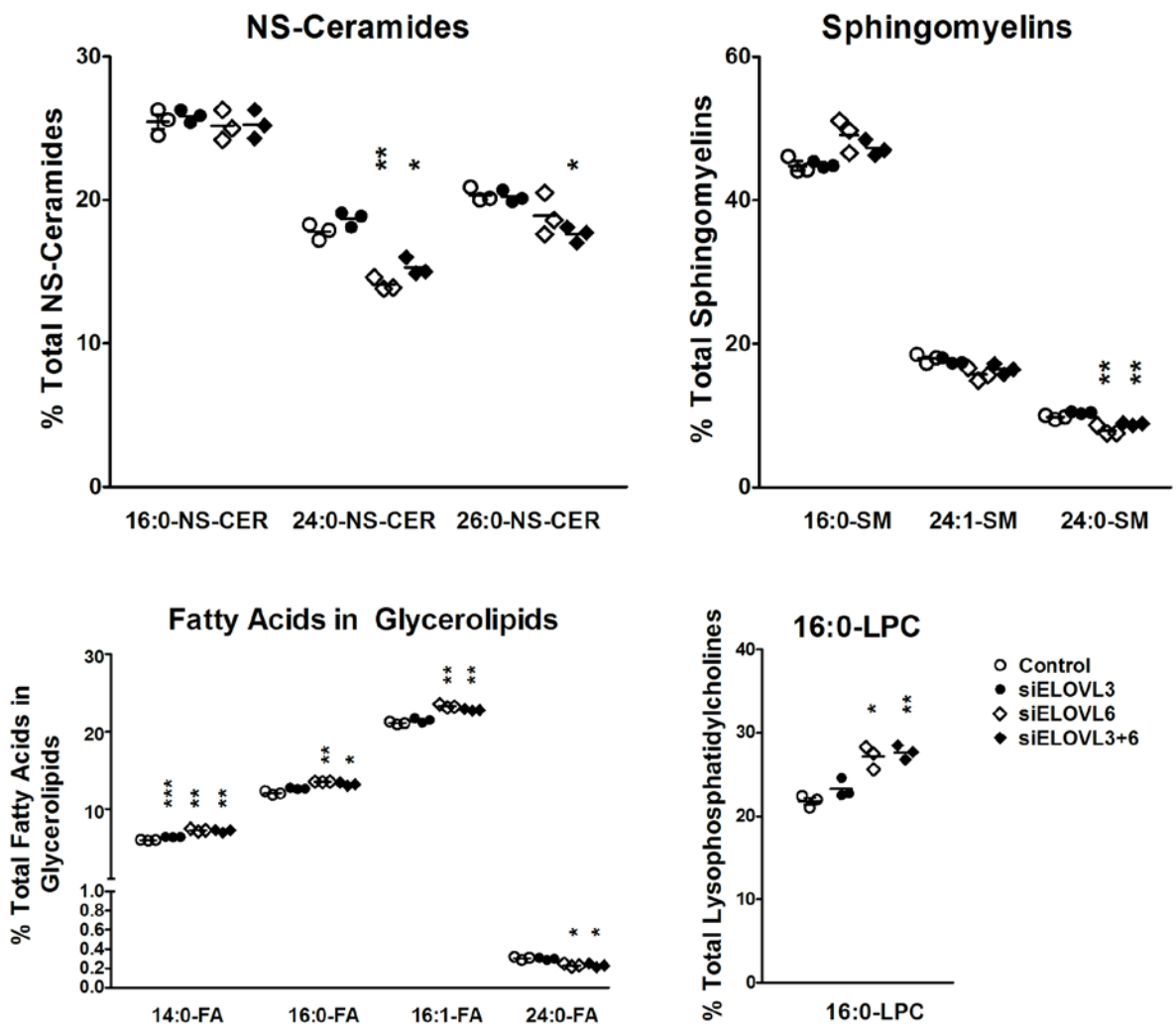

Figure S4. Silencing of ELOVL3 and ELOVL6 results in changes in long-chain and short-chain species within several classes of lipids in Ca^{2+}-differentiated human keratinocytes *in vitro*. Relative proportion of selected species of NS-ceramides with C18-sphingoid base, sphingomyelins, fatty acids in global glycerolipids, and palmitoylglycerolphosphocholine (16:0-LPC) within coresponding classes of lipids is presented. Note that silencing of ELOVL3 and especially ELOVL6 results in the decrease in relative proportion of long chain species in sphingomyelins, NS-ceramides, and lignoceric acids (24:0-FA) while increasing the proportion of short-chain LPC (16:0-LPC) and globally within fatty acids in glycerolipids. * - $p < 0.05$, ** - $p < 0.01$, * - $p < 0.001$ versus corresponding non-targeted siRNA control (two-tailed Student's *t*-test). One of two typical experiments is shown each done in triplicates.